DESIGN STUDY OF RF TRIODE STRUCTURE FOR THE KU-FEL THERMIONIC RF GUN

K. Masuda#, K. Kusukame, T. Shiiyama, H. Zen, T. Kii, H. Ohgaki, K. Yoshikawa, T. Yamazaki,
Institute of Advanced Energy, Kyoto Univ., Gokasho, Uji, Kyoto 611-0011, Japan

Abstract

A coaxial rf cavity with a thermionic cathode on its inner rod has been designed to be adopted in a 4.5-cell rf gun in order to minimize the inherent back-bombardment of electrons onto the cathode. Dependences of the back-bombardment power and the output beam properties on the axial mounting position of the coaxial cavity have been studied using a 2-dimensional simulation code. With an optimal mounting position and phase of ~90 kW rf input fed into the coaxial cavity have shown significant reduction of back-bombardment power of over 80 %. It has also shown a lower longitudinal emittance and a higher peak current of the output beam than the conventional rf gun, while the transverse emittance degradation is reasonably acceptable.

INTRODUCTION

Thermionic rf guns have advantages against photocathode ones, such as low cost, high micropulse repetition rate (high averaged current), and easy operation, which make them well suited for FELs. They however suffer from back-bombardment of electrons onto the thermionic cathode which eventually leads to an output beam energy drop and limits the macropulse duration [1-3]. The back-bombardment effect is seen significant in the 4.5-cell rf gun (Fig. 1 and Table 1) for the KU-FEL linac because of its original design, i.e. a high coupling coefficient, large number of cells, small aperture between the cells. Some countermeasures are applied, such as the use of transverse magnetic fields [4,5] and the temporal control of the rf input for compensating time-varying beam-loading [6-8] with limited successes. The macropulse duration achieved so far is 4 μsec at most for a limited beam output of ~80 mA [8], while a longer duration and a higher current would be desired for the FEL operation.

Numerical studies so far have suggested that the rf triode structure could potentially reduce the back-bombardment power drastically (~80 - 99%) [9,10].

Especially the use of a metal grid for the rf cutoff has shown numerically over 99% reductions of the back-bombardment power without degradation in the output beam properties, by simulations on neglect of the beam scattering by the grid [10,11]. In this work, we investigated an rf triode without a grid for comparison, since the use of a grid is practically undesirable unless it is necessary in terms of the back-bombardment reduction and/or the output beam characteristics.

Also, though the beam properties at the 1.6-cell [9] and the half-cell [10] exits have shown reasonably acceptable degradations or rather enhancements, the beam extraction phase from the rf triode should be considered in adopting it to the 4.5-cell gun, because an off-crest beam injection to the successive cells would lead to a degradation in the output beam transverse emittance due to an increased rf contribution to the emittance growth. In this work, we investigated both the input rf phase and axial mounting position of the coaxial cavity with respect to the main accelerating cells.

#masuda@iae.kyoto-u.ac.jp

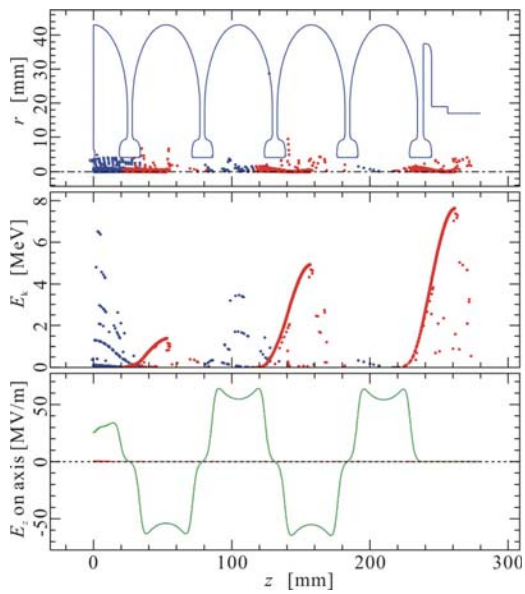

Figure 1: A simulation snapshot showing electrons' radial positions and energies along the longitudinal position, and the on-axis cavity field. The blue dots indicate back-streaming electrons. A 2mm ϕ thermionic cathode with a 30 A/cm^2 current density is located at z = 0, and the cavity voltage is 10 MV to yield 7.6 MeV output.

Table 1: Beam properties by the simulation on neglect of the back-bombardment effect. Only the electrons within an output beam energy spread of $\Delta E_k/E_{k,max}$ = 3 % are taken into account.

at the gun exit	
charge, ΔQ	29.00 pC
peak current, I_{peak}	10.00 A
normalized rms emittance, $\varepsilon_{r,n}$	1.20 π mm mrad
longitudinal rms emittance, ε_z	37.00 psec keV
at the 1st cell exit	
energy spread, $\Delta E_{k1}/E_{k1,max}$	6.60 %
charge, ΔQ_1	29.00 pC
peak current, $I_{1,peak}$	10.40 A
normalized rms emittance, $\varepsilon_{r1,n}$	0.53 π mm mrad
longitudinal rms emittance, ε_{z1}	1.80 psec keV

COAXIAL CAVITY DESIGN

Figure 2 shows the coaxial cavity geometry to be installed in the rf gun instead of the conventional cathode, and the fundamental (2856 MHz) eigenmode pattern by a 2-dimensinal eigenmode solver [12]. The outer radius is limited up to ~15 mm due to the cathode mount geometry in the rf gun. We set it as the maximum, 15 mm to minimize the coupling coefficient, β, between the coaxial cavity and the backside coaxial waveguide from which an rf power is to be fed. The rf cutoff is ensured by a drift tube of 4 mm in diameter and 5 mm in length between the coaxial cavity and the successive half cell.

Figure 3 shows particles' snapshots by a 2-dimensional particle-in-cell simulation code [13] for three different coaxial inner rod geometries on which the same thermionic cathode (2 mmϕ, 30 A/cm^2) as is used in the conventional diode rf gun shown in Fig. 1. The code can reproduce the required rf input, P_{in}, for a given rf voltage, V_0, taking into account the beam-loading effect [3,13].

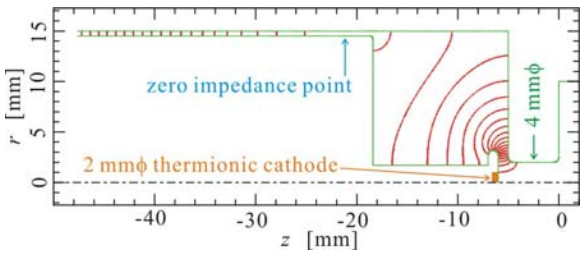

Figure 2: An eigenmode pattern in a coaxial cavity with a thermionic cathode on its inner rod, to replace the cathode in the conventional diode rf gun.

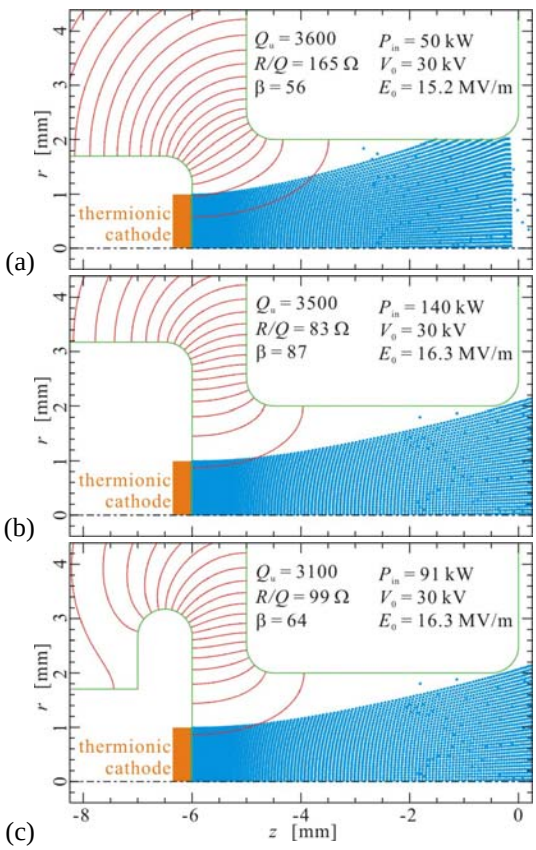

Figure 3: Eigenmode patterns and particle snapshots in the coaxial cavity, comparing three different geometrical designs of the coaxial inner rod. Peak electric field strengths on the cathode (E_0), and required rf input (P_{in}) are shown for a fixed peak cavity voltage, V_0 = 30 kV.

In the design (a), the beam tends to hit the drift tube due to radial forces by both the rf and the space charge. The geometry (b) shows a good beam transport because of a reduced radial rf field, while at the same time the larger inner rod diameter increases β, leading to a higher P_{in} requirement for a fixed V_0. Finally, the design refinement in (c) meets both the requirements, showing a good beam transport and an acceptably high field with a moderate P_{in} below 100 kW, the maximum available power in our experiments scheduled in the near futere.

BACKBOMBARDMENT AND BEAM PROPETIES BY THE TRIODE RF GUN

In the simulations in the triode rf gun, we varied the axial mounting position, z_0, of the coaxial cavity with respect to the main accelerating cells in the 4.5-cell rf gun (see Fig. 4), as well as the rf voltage, V_0, and phase, $\Delta\phi_{01}$, in the coaxial cavity. The cavity voltage in the main accelerating 4.5 cells is fixed as 10 MV throughout.

As seen in Fig. 4, the 1st half cell geometry is slightly changed as the z_0 varies, so that its resonant frequency, quality factor and shunt impedance remain unchanged.

The back-bombardment effect is neglected, i.e. the cavity voltages and the cathode current density are kept constant until periodically steady-state solutions.

Back-Bombardment Power and Beam Properties at the First Cell Exit

Figure 5 and 6 show back-bombardment power onto the 2 mmϕ cathode, P_{back}, bunch charge, ΔQ_1, and transverse normalized rms emittance $\varepsilon_{r1,n}$ at the 1st half cell exit. For comparisons, they are normalized by those in the conventional diode rf gun listed in Table 1. Electrons

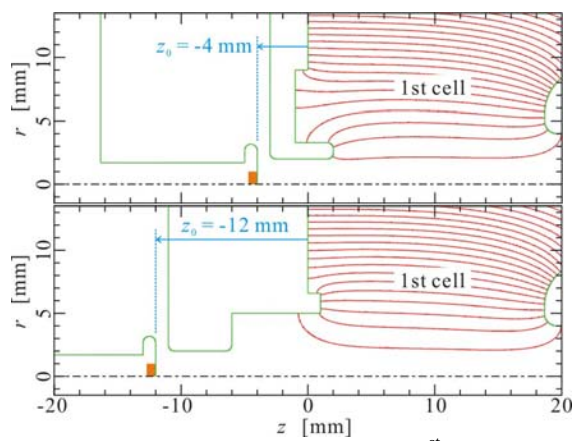

Figure 4: Eigenmode patterns of the 1st cell for two different mounting positions (z_0) of the coaxial cavity. In the conventional diode rf gun (see Fig. 1 and Table 1) the cathode is located at z = 0.

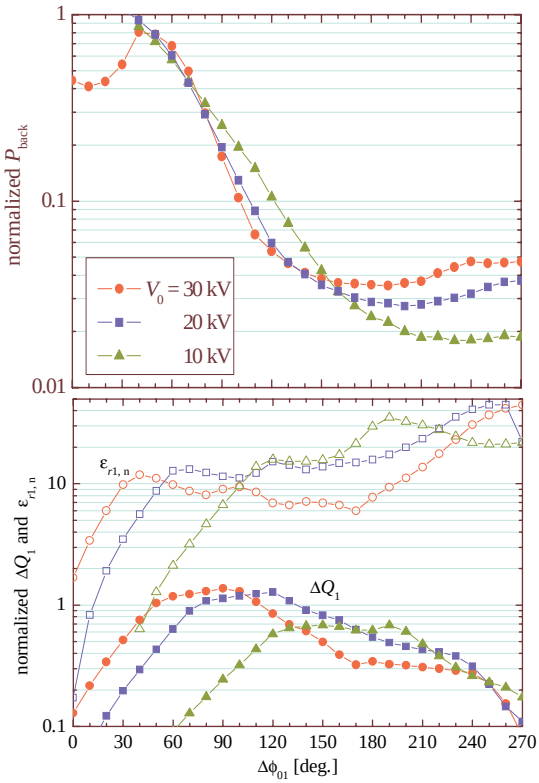

Figure 5: Back-bombardment power (P_{back}), bunch charge and transverse normalized rms emittance at the 1st cell exit (ΔQ_1 and $\varepsilon_{r1,n}$) divided by those in the conventional diode rf gun (see Table 1), as functions of $\Delta\phi_{01}$ and V_0 for z_0 = -4 mm.

within an energy spread of $\Delta E_{k1}/E_{k1,max}$ = 6.6 % are taken in account in the ΔQ_1 and $\varepsilon_{r1,n}$, since they are found contribute to an acceptable output beam energy spread of $\Delta E_k/E_{k,max}$ = 3 % for the case of the conventional diode rf gun shown in Fig. 1 and Table 1.

As seen in Fig. 5, a lower V_0 results in a lower ΔQ_1 and larger $\varepsilon_{r1,n}$ without significant reduction of P_{back}. Thus V_0 is fixed as the maximum, 30 kV hereafter.

In comparison with the use of a metal grid instead for the rf cutoff [10], the existence of zero-field region in between the cathode and the 1st half cell is found result in higher P_{back}, while the reduction of P_{back} by the present rf triode is still significant.

In Fig. 6, regardless of the phase control by z_0, $\phi_{1,head}$ is found far ahead of the crest for $\Delta\phi_{01}$'s where the P_{back} reduction is over 90 % (called operational mode (I) hereafter).

At a lower $\Delta\phi_{01}$, however, a local minimum of P_{back} is found, which is seen to reach 80 % reduction for z_0 = –6, –8 and –10, and is also seen to shift in terms of $\Delta\phi_{01}$ as z_0 decreases. Thus P_{back} at $\phi_{1,head}$ = 1 π rad (crest) decreases with decreasing z_0 as shown in Fig. 7. This operational mode (II) is not seen in the grid-based rf triode [10], which corresponds virtually to z_0 = ~ –1 mm.

Note that, in the conventional rf gun, $\phi_{1,head}$ is 0.94 π rad, slightly ahead of the crest as shown in Fig. 6, because the rf voltage and corresponding output energy of 7.6

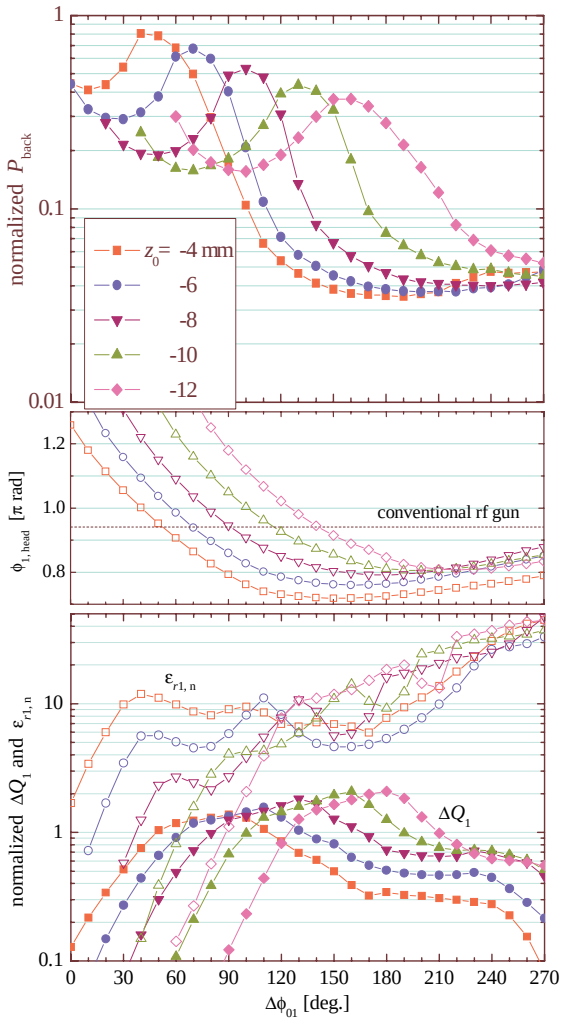

Figure 6: P_{back}, ΔQ_1 and $\varepsilon_{r1,n}$ divided by those in the conventional diode rf gun, and bunch head phase through the 1st cell exit ($\phi_{1,head}$), as functions of $\Delta\phi_{01}$ and z_0 for V_0 = 30 kV.

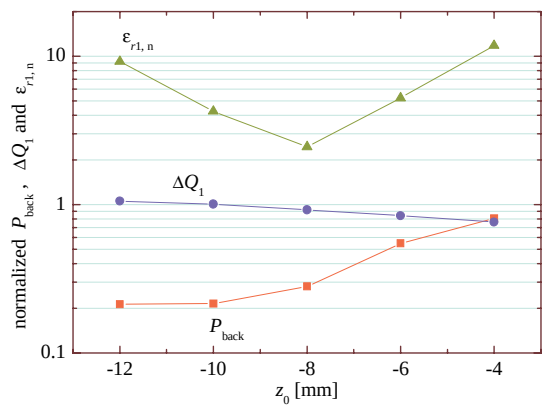

Figure 7: P_{back}, ΔQ_1 and $\varepsilon_{r1,n}$ divided by those in the conventional diode rf gun for $\Delta\phi_{01}$ where $\phi_{1,head}$ = 1 π rad, as functions of z_0 for V_0 = 30 kV.

MeV is higher than the nominal value of 5 MeV. Nevertheless we usually operate the gun at a higher energy, since it results in a lower beam emittance.

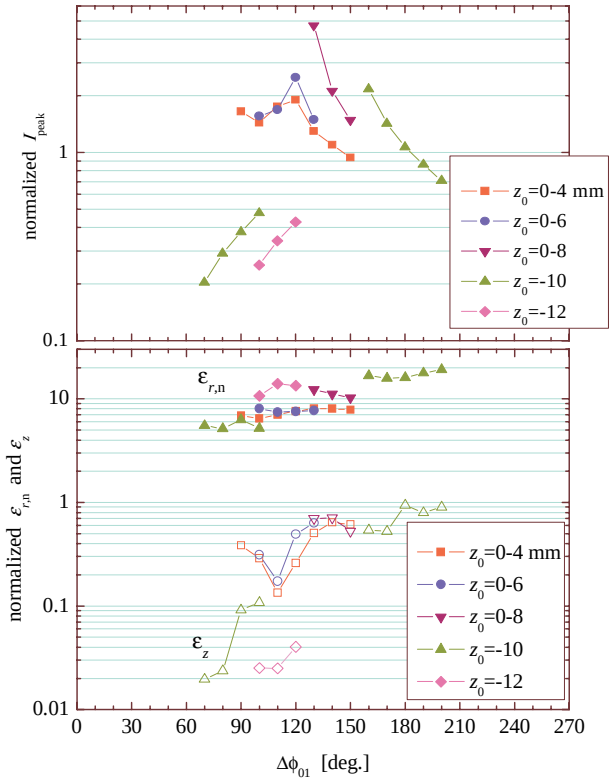

Figure 8: Dependences of the output beam properties on $\Delta\phi_{01}$ and z_0.

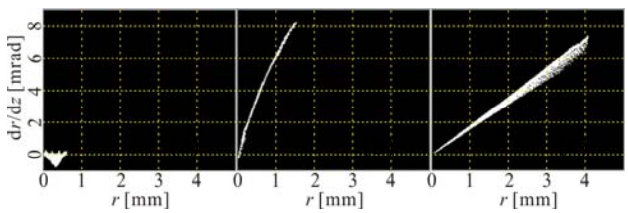

Figure 9: Transverse phase space distributions of the output beams by (a) the conventional diode gun, the triode gun with (b) z_0 = –10 mm, $\Delta\phi_{01}$ = 100 deg. (mode (II)), and (c) z_0 = –6 mm, $\Delta\phi_{01}$ = 120 deg (mode(I)).

Table 2: Comparisons of back-bombardment powers and output beams' properties between the conventional diode and the triode rf guns.

	P_{back} [kW]	I_{peak} [A]	$\varepsilon_{r,n}$ [π mm mrad]	ε_z [psec keV]
conventional diode rf gun	21.0	10.0	1.2	37.0
z_0 = –10 mm, $\Delta\phi_{01}$ = 100 deg.	04.3	04.9	6.3	04.0
z_0 = 0–6 mm, $\Delta\phi_{01}$ = 120 deg.	01.6	26.0	9.1	18.0

Output Beam Properties

Figure 8 shows output beam properties for $\Delta\phi_{01}$'s and z_0's where the reduction of P_{back} is found over 80 % in Fig. 6, in both modes (I) and (II). Figure 9 and Table 2 show the output beams at optimal $\Delta\phi_{01}$'s and z_0's in terms of $I_{peak}/e_{r,n}^2$ for the modes (I) and (II), together with the output by the conventional diode rf gun.

The off-crest beam injection in the mode (I) is found to result in larger emittances than the mode (II) in exchange of higher peak currents. It should be noted that the mode (I) greatly reduces the rf contribution to the transverse emittance growth, i.e. the beam is obviously seen narrow in the phase space in Fig. 9(b), because of the optimal beam injection phase into the 2nd full cell. In comparison with the conventional rf gun, though the rf contribution is seen much reduced in the mode (II), transverse emittance is rather degraded by the radial rf field nonlinear to the radial position, i.e. the phase space distribution is seen bent much in Fig. 9(b). In the longitudinal emittance, improvements are seen in both modes (I) and (II).

CONCLUSIONS

The present rf triode structure has shown significant reductions of the back-bombardment power, and reduced longitudinal emittances and enhanced peak currents of the output beam. The optimal axial position of the coaxial cavity with respect to the main cells has shown a greatly reduced rf contribution to the transverse emittance growth by controlling the beam longitudinally with respect to the rf. Transversely, however, the present design yields a larger beam radius, eventually leading to a transverse emittance growth due to the contribution by the nonlinear radial rf fields. Though the transverse emittance degradation is reasonably acceptable, the wehnelt configuration and/or optimal control of the rf voltages should be considered in order to induce radial beam focusing to minimize the output transverse emittance.

REFERENCES

[1] C.B. McKee, et al., Nuclear Instruments and Methods in Physics Research A **304** (1991) 386.
[2] T. Kii, et al., Nuclear Instruments and Methods in Physics Research A **475** (2001) 588.
[3] K.Masuda, et al., Nuclear Instruments and Methods in Physics Research A **483** (2002) 315.
[4] T. Kii, et al., Proc. 9th Intnl. Conf. Synchrotron Radiation Instrumentation, May 2006, in press.
[5] C.B. McKee, et al., Nuclear Instruments and Methods in Physics Research A **296** (1990) 716.
[6] T. Kii, et al., Nuclear Instruments and Methods in Physics Research A **507** (2003) 340.
[7] F. Li, et al., Nuclear Instruments and Methods in Physics Research A **407** (1998) 332.
[8] T. Kii, et al., Proc. FEL2005 (2006) 584.
[9] K. Kanno, et al., Japanese Journal of Applied Physics **41**-1 (2002) 62.
[10] K. Masuda, et al., Proc. FEL2005 (2006) 588.
[11] K. Kusukame, master thesis Kyoto Univ., 2006 (in Japanese).
[12] K. Masuda, et al., IEEE Transaction on Microwave Theory and Techniques **46**-8 (1998) 1180.
[13] K.Masuda, Ph,D. thesis Kyoto Univ, 1997.